Journal of Materials Chemistry A

Accepted Manuscript

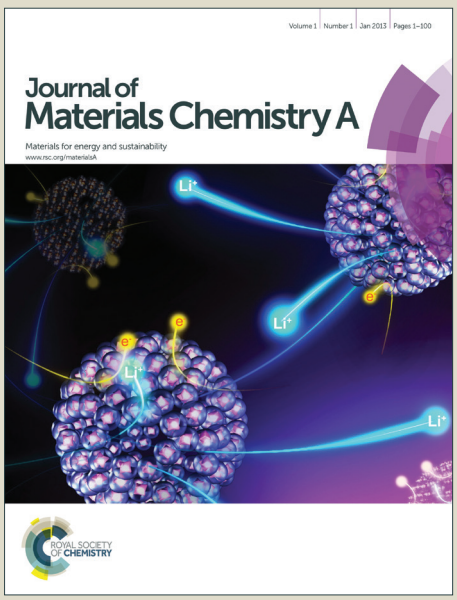

ROYAL SOCIETY OF CHEMISTRY

www.rsc.org/materialsA

Journal of Materials Chemistry A

PAPER

The effect of solid electrolyte interphase on the mechanism of operation of lithium-sulfur batteries.

Received 00th January 20xx,
Accepted 00th January 20xx

DOI: 10.1039/x0xx00000x

www.rsc.org/

E. Markevich*[a], G. Salitra*[a], A. Rosenman[a], Y. Talyosef[a], F. Chesneau[b] and D. Aurbach*[a]

Composite sulfur–carbon electrodes were prepared by encapsulating sulfur into the micropores of highly disordered microporous carbon with micrometer-sized particles. The galvanostatic cycling performance of the obtained electrodes was studied in 0.5M Li bis(fluorosulfonyl)imide (FSI) in methylpropyl pyrrolidinium (MPP) FSI ionic-liquid (IL) electrolyte solution. We demonstrated that the performance of Li–S cells is governed by the formation of solid electrolyte interphase (SEI) during the initial discharge at potentials lower than 1.5V *vs.* Li/Li^+. Subsequent galvanostatic cycling is characterized by one plateau voltage profile specific to quasi-solid-state reaction of Li ions with sulfur encapsulated in the micropores in solvent deficient conditions. The stability of the SEI thus formed, is critically important for the effective desolvation of Li ions participating in quasi-solid-state reactions. We proved that realization of the quasi-solid-state mechanism is controlled not by the porous structure of the carbon host but rather by the nature of the electrolyte solution composition and the discharge cut off voltage value. The cycling behavior of these cathodes is highly dependent on sulfur loading. The best performance can be achieved with electrodes in which the sulfur loading was 60% by weight, when sulfur filled micropores are not accessible for N_2 molecules according to gas adsorption isotherm data. A limited contact of the confined sulfur with the electrolyte solution results in the highest reversible capacity and initial Coulombic efficiency. This insight into the mechanism provides a new approach in the development of new electrolyte solutions and additives for Li-S cells.

Introduction

Lithium-sulfur batteries have been the subject of very intensive work throughout the world in recent years due to the high theoretical specific capacity of sulfur cathodes (1672 mA h g^{-1}) which is an order of magnitude higher than that of lithiated transition-metal oxide and phosphate cathode materials used in commercial Li-ion batteries (140-200 mA h g^{-1}) [1-5]. This high capacity is due to the ability of sulfur atoms to accept two electrons resulting in the conversion of elemental sulfur to lithium sulfide (Li_2S) in an ideal cell. Furthermore, sulfur is non-toxic, environmentally friendly, naturally abundant, easily available and relatively cheap.

The chemistry of Li-S electrodes differs drastically from that of Li-insertion cathodes. During the first discharge, molecules of elemental sulfur S_8 accept electrons and turn to a chain of electroactive Li-polysulfides that are soluble in most commonly used solvents and diffuse freely throughout the cell to the anode side. The dissolved long-chain polysulfides (Li_2S_m, m=4–8) may be continuously reduced at the Li-metal anode during cell charging and thereby they can never be fully oxidized the cathode. This phenomenon known as the "shuttle mechanism" is a critical problem of Li–S cells which leads to their low columbic efficiency, i.e. only a partial realization of the full capacity of the sulfur cathodes and a fast capacity fading [6].

Intensive research efforts have focused on preventing the shuttle process. The use of porous carbons with high adsorption capacity and good conductivity enables sulfur encapsulation and polysulfides trapping in the pores [7-9]. Adsorption or chemisorption of polysulfide anions by metal oxides [10-13], silica [14], 2D MXene conductive nanosheets [15] enhance the stability of sulfur cathodes. Another strategy aiming to suppress the shuttle process is the use of electrolyte solutions in which the polysulfide species are insoluble, for example, ionic liquid electrolytes (IL) [16, 17]. Park et al. [17] showed that Li_2S_m dissolution was effectively suppressed in the IL electrolytes with bis(trifluoromethylsulfonyl)imide (TFSI) anions and demonstrated reversible cycling of S–C composite electrodes. They also concluded that fast capacity fading observed for Li–S cells in IL electrolytes containing bis(fluorosulfonyl)imide (FSI) anions is the result of decomposition of these anions, because of their reaction with polysulfides. However, in our recent work [18] we demonstrated stable performance of Li–S cells using IL electrolyte solutions with FSI anions and showed that the structure of the carbon matrix plays a key role in determining the performance of the cells. For LiFSI/MPP FSI electrolyte

[a] Department of Chemistry Bar-Ilan University, Ramat Gan 52900 Israel. E-mail: markeve@biu.ac.il, salitrg@biu.ac.il, Doron.Aurbach@biu.ac.i
[b] BASF SE, Ludwigshafen 67056, Germany.

Electronic Supplementary Information (ESI) available: Sulfur-carbon composite characterization results: XRD, TGA, HRSEM and cathode performance (CV and galvanostatic cycling). See DOI: 10.1039/x0xx00000x

solutions high performance of Li–S cells with a capacity approaching their theoretical values was demonstrated when the hosting carbon matrix was fully desorbed micrometer sized activated carbon denoted as AC1, and very poor performance was observed for S-C composite prepared with nanosized BP2000 carbon. To the contrary, for LiTFSI/butylmethyl pyrrolidinium (BMP)TFSI electrolyte solutions S-C composite cathodes exhibited a reversible behavior in accordance to [17]. It should be pointed out that the voltage profile observed for S-AC1 cathodes in the FSI-based electrolyte solutions differed from that typically observed for S–C electrodes. Typical voltage profiles of sulfur cathodes characterized by two discharge plateaus at about 2.4 and 2.0V and one charge plateau at approximately 2.3 were observed in the majority of cases described in the literature. The voltage profiles measured for S-AC1 cathodes in FSI-based electrolyte solutions exhibit a single discharge plateau at 1.7V and a corresponding charge plateau at about 2V. Similar voltage profiles were observed only for limited cases of S-C cathodes cycled mainly in organic carbonate based electrolyte solutions [7, 19-25], as well in some ethereal electrolyte solutions [26, 27]. Analogous single-plateau voltage profiles were also observed for sulfurized carbon cathodes with covalently bonded sulfur in organic carbonate electrolyte solutions [28, 29], as well as for all-solid-state Li-S batteries with superionic sulfide cathode Li_3PS_{4+n} and Li_3PS_4 solid electrolyte [30, 31].

In this work, we report on the effect of sulfur loading and the role of SEI which is formed on the surface of S-AC1 encapsulation cathodes during the operation of Li-S cells in FSI-based IL electrolyte solutions. We propose a mechanism for reversible lithiation of S-C cathodes in different electrolyte solutions which explains well the two types of the voltage profiles observed for different Li-S cells. We also discuss the effect of the electrolyte solutions, cycling conditions and carbon matrix used on the voltage profile and related mechanism. This work can promote development of highly effective and relatively cheap high capacity composite sulfur cathodes.

Experimental

Micrometer-sized activated carbon powder (AC1) from Mead Westvaco, USA (Figure 1S a and b) was heated at 950 °C for 5 h under 95% Ar 5% H_2 in order to remove oxygen containing groups. Elemental sulfur (Aldrich) and carbon powders were mixed thoroughly by grinding them in mortar and Vortex mixer with various sulfur loading of 40, 50 and 60 wt. %. Then the powders were sealed in a stainless steel vessel (Swagelok) in an argon-filed glovebox and heated for 6 h at 200^0C. The uniformity of sulfur distribution in the sulfur–carbon composite powders thus obtained and the sulfur–carbon composite electrodes is clearly seen from EDX mapping shown in Fig. 1S a, b and Fig. 2S a, b.

BMP TFSI (>98.5%) and Li TFSI (99.95%) were purchased from Aldrich. MPP FSI (>99.9%) was purchased from Solvonic (France) and Li FSI (>99.95%) from Suzhou Fluolyte Co, Ltd (China).

BMP TFSI and MPP FSI before use were dried in vacuum at 80 °C for 20 h, and the water content after drying was 10 ppm for BMP TFSI and 5ppm for MPP FSI. The water content in the ILs was determined by a Karl Fischer titration. Li TFSI and Li FSI were dried in vacuum at 120 °C for 20 h. 0.5M Li TFSI in BMP TFSI, 0.5M Li TFSI in MPP FSI and 0.5M Li FSI in MPP FSI were used as the electrolyte solutions for the electrochemical measurements.

The composite AC1 carbon-sulfur powders, carbon black – Super P (Superior Graphite) and PVdF in a weight ratio of 80:10:10, were mixed with N-methyl-2-pyrrolidone (NMP). Electrodes were prepared by coating the slurry onto aluminum foils using a doctor-blade technique, dried overnight at room temperature in dry air and after then were heated overnight at 60° C in vacuum.

Electrodes of 14 mm in diameter were assembled in a two-electrodes configuration using standard coin-type cells (2325, NRC, Canada) *vs.* Li metal foil with IL electrolyte solutions. The electrodes and separators were impregnated with minimal volume of the electrolyte solution under vacuum. Whatman high purity quartz (SiO_2) microfiber filters or SiO_2 containing polyolefin separators from Entek (USA) were used as separators.

Thermal gravimetric analysis (TGA) was carried out by a TA Instruments apparatus (1GA Q500 model) up to 800°C (10°C min^{-1}, N_2 atmosphere, 10 mL min^{-1}. The samples were pre-heated at 60°C under nitrogen in order to lower their total moisture content. The elemental analysis was carried out by an elemental analyzer (Flash EA 1112, Thermo Fischer Scientific).

The sulfur loading per electrode was 1.1 - 1.4 mg. The sulfur content in the composite sulfur-carbon powder determined by TGA (Figure S3 in the Supporting Information) and elemental analysis comprised 40,50 and 60 wt. %.

Coin-cells were cycled using a computerized multi-channel BT2000 battery cycler (Arbin Instruments**).** Nitrogen adsorption isotherms were measured using Autosorb iQ2 (Quantachrome) at 77 K. Cyclic voltammograms and electrochemical impedance spectra were measured using a potentiostat-galvanostat Model 128N Autolab equipped with FRA-2 , Eco Chemie using standard coin-type cells (2325, NRC, Canada) assembled in three electrodes configuration as described in [32].

X-ray diffraction (XRD) patterns were obtained with a D8 Advance system (Bruker Inc.) using Cu Kα radiation operated at 40 mA and 40 kV.

HRSEM images and EDS data were obtained using a FEI xHR-SEM Magellan 400L microscope, equipped with the Oxford Industries INCAx-sight energy dispersive spectrometer (EDS) attachment. EDS measurements and mapping were performed at an operating voltage of 5 kV.

XPS measurements were performed with a 5600 Multi-Technique System (Physical Electronics, USA) with a monochromatic Al Ka radiation (1486.6 eV). High-resolution measurements of the target elements were done with path energy of 11.75 eV.

Air sensitive electrodes after cycling were transferred from the glovebox to the microscope and X-ray photoelectron spectrometer without contact with ambient air.

Results and discussion

In our recent communication we showed that Li–S cells, with composite S–C cathodes prepared with activated carbon (denoted as AC1), using 0.5M LiFSI/MPPFSI IL electrolyte solution may be reversibly cycled with a high capacity and very high cycling efficiency at 60°C. The updated data related to the prolonged cycling of Li-S/AC1 cells is shown in Fig.1a. After 200 cycles at 60°C the discharge capacity of the cells exceeded 840 $mAhg^{-1}$ with a Coulombic efficiency > 99% (black curve). It is significant that this reversible behavior can be realized only after necessary pretreatment through repeated charge/discharge cycling with a discharge cutoff value of 1.4V *vs.* Li/Li^+ at 30°C, as is shown in Fig.1c. In the first discharge down to 1.4V a plateau at about 1.5-1.4V *vs.* Li/Li^+ develops which disappears during subsequent 1-2 cycles, resulting in reversible cycling with a single discharge and charge plateaus observed at about 2.0 and 2.1V *vs.* Li/Li^+, respectively (Fig. 1 c, d). Thus, voltage profile with a potential hysteresis was observed, which is very similar to that observed in [7, 19-25] in the case of organic carbonates based electrolyte solutions. The limitation of the discharge cut off value to 1.7V *vs.* Li/Li^+ results in a reversible cycling of the identical cells with a very low reversible capacity of about 40 mA h g^{-1} with voltage profiles commonly observed for Li-S cells, namely, with two discharge plateaus at about 2.3 and 2.1V *vs.* Li/Li^+ and a single charge plateau at 2.25V *vs.* Li/Li^+ (Fig. 1b). This type of behavior is probably observed due to the activity of the little portion of sulfur which is not confined in the micropores and remains on the surface of the carbon particles.

Interestingly, no activity was observed for S/AC1 electrodes in identical cycling conditions (discharge cut off value of 1.4V) when we used IL electrolyte solution with TFSI anions (Fig. 1a, blue curves). Thus, the reactivity of FSI anion at a potential lower than 1.5V-1.4V *vs.* Li/Li^+ leads to the development of a potential plateau in the initial discharge which is a necessary pretreatment condition for the subsequent stable cycling.

It should be mentioned that cycling results presented in Fig.1 relate to 50 wt.% of sulfur in S/AC1 composites. In this case the free pore space comprised 0.06 cc g^{-1}. To realize the effect of sulfur loading and the remaining free pore space on the performance of S/AC1 composite electrodes we prepared a series of electrodes with sulfur loading of 40, 50 and 60 wt.%. Fig. S3 shows the TGA curves of sulfur-AC1 powders with 40, 50 and 60 wt. % sulfur, with weight losses which correspond exactly to the sulfur content in these composite powders. X-ray diffraction patterns of AC1 pristine powder, elemental sulfur powder and composite AC1-sulfur powders with different wt. % of sulfur are shown in Fig. S4.

The N_2 adsorption/desorption isotherms related to AC1 samples before impregnation and AC1-S composite powders measured at 77 K are shown in Fig. 2a, and the cumulative pore size distributions are shown in Fig. 2b. The type I isotherm obtained for AC1 pristine powder indicates the microporous structure of this carbon (≤2nm) and its relatively

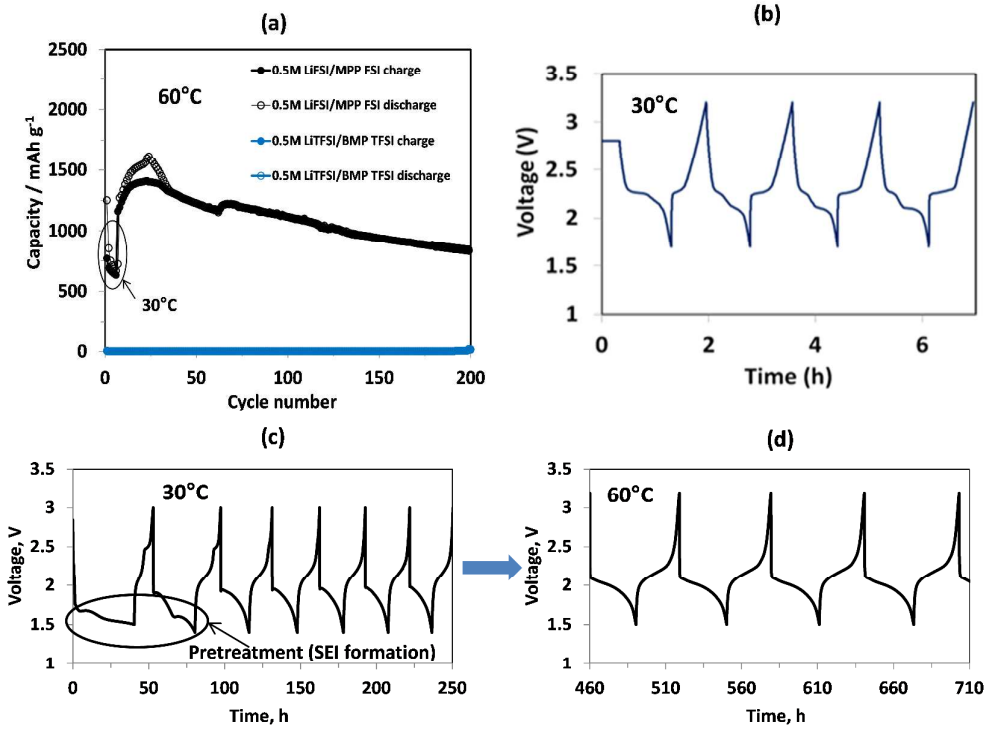

Fig.1. Charge (filled dots)/discharge (hollow dots) curves measured for composite S–C electrodes (50 wt.%S) in 0.5M Li FSI in MPP FSI (black curves) and 0.5M Li TFSI in BMP TFSI (blue curves) electrolyte solutions (a), voltage profile of Li – S cells at 30°C with lower cut-off value of 1.7V (b), voltage profile of Li – S cells measured during the pretreatment step and following galvanostatic cycling of Li – S cells at 30°C with lower cut-off value of 1.4V (c) and galvanostatic cycling of Li – S cells at 60°C with lower cut-off value of 1.5V (d). Current density: 50 mAg^{-1} sulfur.

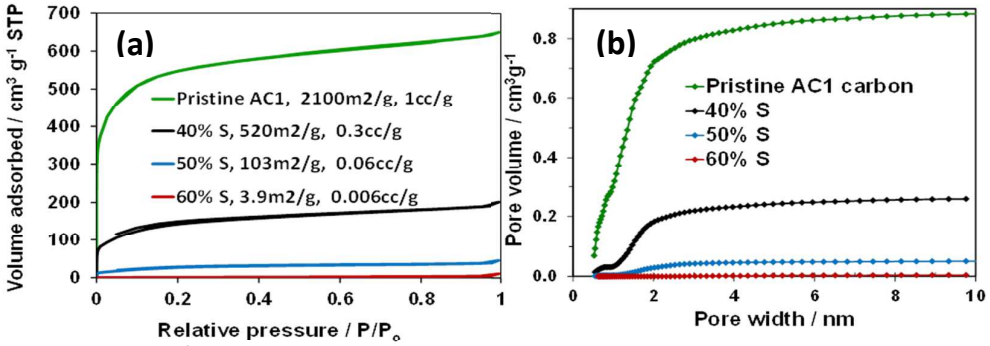

Fig.2. N2 adsorption/desorption isotherms measured at 77K (a) and cumulative pore size distributions calculated by DFT (b) of pristine AC1 carbon powder and AC1 impregnated with 40, 50 and 60 wt% of sulfur,

low external surface area. BET specific surface area and the total pores volume of the AC1 powder before and after impregnation with 40, 50 and 60 wt.% sulfur at $P/P_0 = 0.90$ are presented in Fig. 2a. It is seen that the BET specific surface area after infiltration of 60 wt. % S comprised 3.9 m^2g^{-1} only, and the total pores volume was 0.006 cc/g. This means that for the AC1-S composite powder with 60 wt.% S there is no more pores accessible for N_2.

Galvanostatic cycling performance of Li-S cells in LiFSI/MPPFSI electrolyte solutions at 30°C with S-AC1 cathodes prepared with these three composite powders are shown in Fig.3. It should be noted that commonly used polyolefin separators are

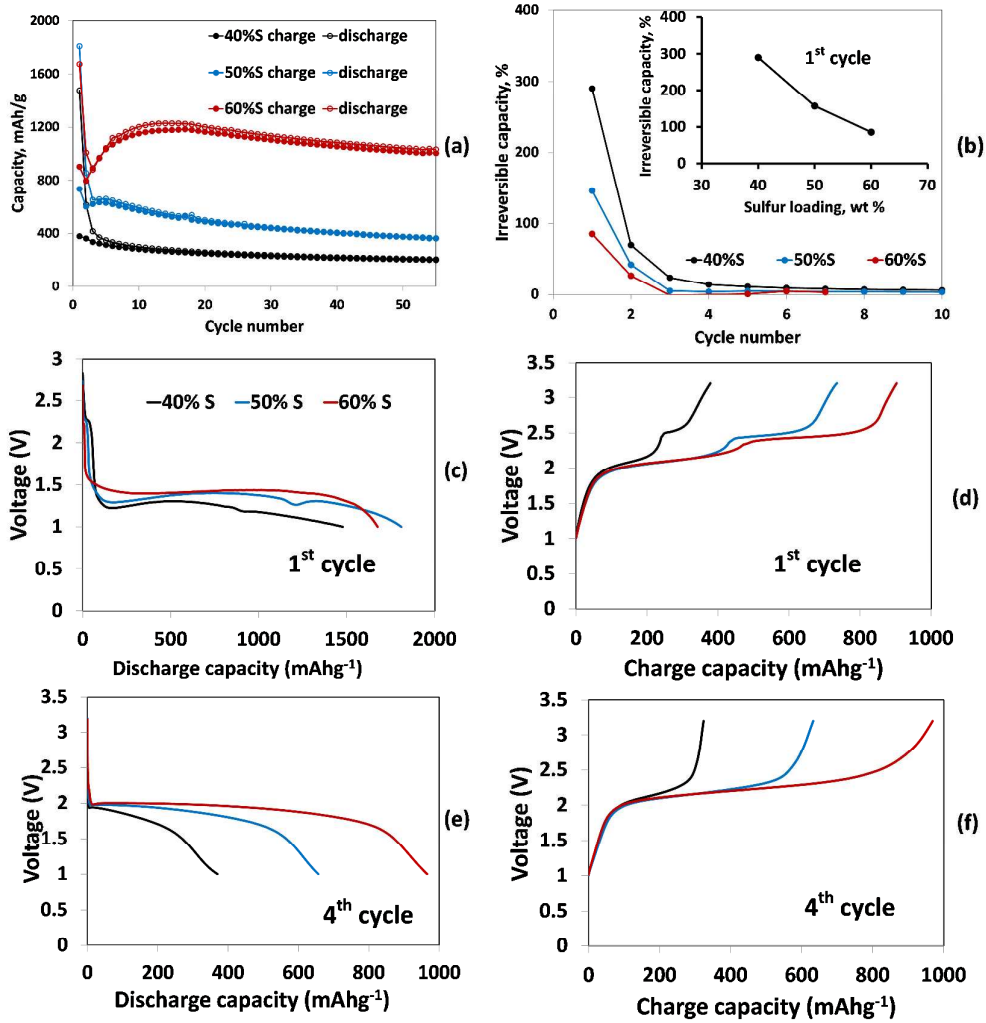

Fig.3. Galvanostatic cycling results obtained for Li-S cells with S-AC1 cathodes with different wt% of sulfur, as indicated. (a) Galvanostatic charge-discharge curves, (b) irreversible capacity vs. cycle number Insert: Initial irreversible capacity measured as a function of sulfur loading,(c-f) voltage profile measurd during discharge (c, e) and charge (d, f) steps in the 1st (c, d) and the 4th (e, f) galvanostatic cycles. 30°C. Current density 50 mA g^{-1}.

poorly wetted in IL electrolytes. For this reason the results shown in Fig.3 were obtained with cells in which SiO_2 containing polyolefin separators from Entek were used, whereas the results shown in Fig.1 (prolonged cycling at 60°C) relate to cells with quartz separators. We revealed that at room temperature the use of the quartz separator is complicated by the fact that during the prolonged cycling the formation of Li dendrites and their penetration through the separator was observed (Fig. S5). As one can see from the voltage profiles of such cells, the growth and penetration of dendrites occur generally during the charge step when Li deposition on the Li metal counter electrodes occurs. Comparison of the 3 types of separators in the IL electrolyte solutions demonstrates a much lower resistance of the separators from Entek compared to polypropylene separators (Supplementary Information, Fig. S6), and the polyethylene separators which cannot be wetted at all in the IL based solutions. Thus, the use of composite separators as those produced by Entek, enables cycling of the Li-S/AC1 cells at room temperature.

As is seen from Fig. 3a, as the sulfur loading was higher, so the cycling behavior observed was better and the irreversible capacity measured in the initial galvanostatic cycle was lower as well (Fig. 3b, insert). Again, as for the cell presented in Fig. 1, the voltage profiles of the cells measured in the 1st galvanostatic cycle (Fig. 3c, d), differ substantially from that measured in the subsequent cycles (Fig. 3e, f). One can observe that during the initial discharge process, the potential plateau at 1.5-1.2V (depending on the electrode composition) is much longer than the similar potential plateaus measured in the following cycles (about 1.7-2V). Cycling voltammograms recorded during four initial cycles of S-AC1 cathodes (60 wt.%S) fully correspond to the galvanostatic curves shown in Fig.3 and demonstrate a voltage hysteresis phenomenon Fig. S7.

We anticipate that the low voltage plateau in the first discharge process corresponds to the formation of protective surface films on the S-AC1 electrodes. To confirm this suggestion we performed surface analysis to cycled S/AC1 electrodes.

Fig. 4 presents SEM images of a pristine composite S-AC1 electrode and S-AC1 electrodes cycled with different discharge cut off values, fully charged and rinsed with dry DME. EDS data obtained from the locations marked with the frames in Fig. 4 are summarised in Table 1. It is seen, than the surface of the pristine electrode (Fig. 4a) does not differ from that of the electrode cycled down to 1.7V (Fig. 4b) and no surface films on the carbon particles are observed after this cycling procedure. The EDS results indicate disappearance of sulfur from the surface of the particles of the cycled electrodes, obviously, as a result of rinsing the cycled electrodes with DME. Remarkably, the PVdF binder is present on the surface of large carbon particles only in very low quantity. For this reason, in order to minimize the masking effect of PVdF and carbon black particles on the response coming from the surface films, we collected EDS spectra from sites located on the surface of large carbon particles. It is clearly seen, that the surface of the electrodes

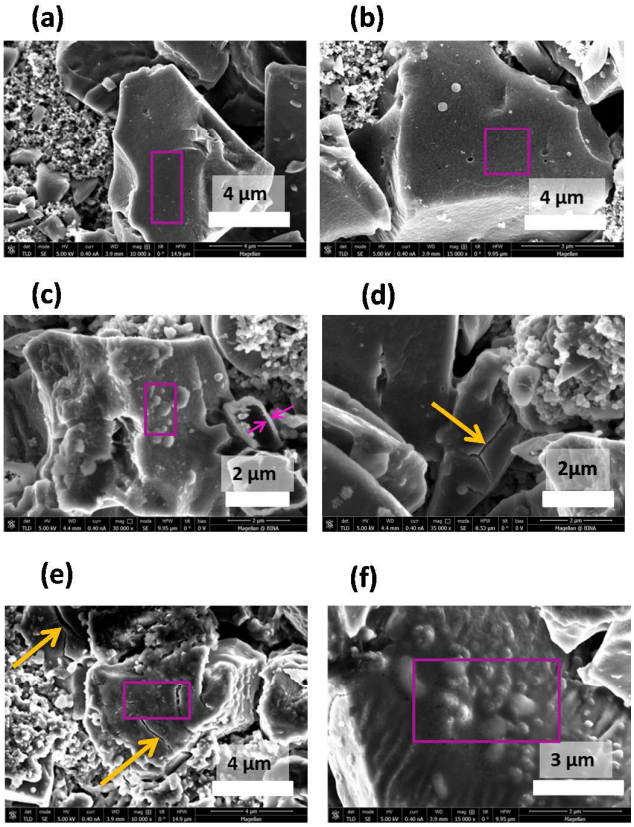

Fig.4. SEM images of composite S-AC1 electrodes.
(a) pristine electrode, (b) electrode cycled at 30°C with lower cut off value of 1.7V, (c) and (d) electrodes cycled at 30°C with lower cut off value of 1V, (e) and (f) two different locations of the electrode cycled at 60°C with lower cut off value of 1V. The frame indicates the locations from which EDS spectra were collected.

cycled down do 1V during discharge is covered with surface films (Fig. 4c-f). The thickness of this film estimated for electrode cycled at 30°C from SEM image (Fig. 4 c) is about 0.2 µm. This observation is supported by the EDS results, which reveal the decrease in the atomic % of carbon and the appearance of nitrogen containing species on the surface. The increase in the atomic concentrations of oxygen, fluorine and sulfur suggests that the main components of these films may contain the products of the reduction of FSI anions. The surface concentration of these species is obviously higher for the electrodes cycled at 60°C. It is seen, that C/S particles in the composite electrodes cycled down to 1V underwent cracking (yellow arrows in Fig. 4d and e) due to a large volume expansion of sulfur during its lithiation process. It is clear, that the free pore volume of C/S is not enough to accommodate Li_2S which is formed during the sulfur reduction process, and breaking open of the pores and particles structure is observed. However, the highest reversible capacity at room temperature was achieved for the electrodes with the highest sulfur loading of 60%. Cracking of the particles is obviously responsible for the increase of the capacity during the initial cycling.

Table 1. Atomic concentrations measured by EDS for sulfur-AC1 pristine composite electrodes and electrodes cycled in 0.5M LiFSI/MPPFSI electrolyte solution and rinsed with dry DME.

Element	Pristine AC1-S composite electrode (Fig. 4a)	AC1-S composite electrode after 5 cycles between 1.7 and 3.2V at 30°C (Fig. 4b)	AC1-S composite electrode after cycling between 1 and 3.2V at 30°C (Fig. 4c)	AC1-S composite electrode after cycling between 1 and 3.2V at 60°C	
				(Fig. 4e)	(Fig. 4f)
C	71.02	96.00	67.59	58.18	44.69
N	-	-	1.32	1.78	3.18
O	1.53	1.52	13.82	16.77	26.63
F	0.66	0.57	9.19	6.11	10.14
S	26.79	1.91	8.08	17.16	15.37

Recently Kim et al. [33] reported on the *in-situ* formation of passivating layer on S/C electrodes surfaces in LiFSI/dimethoxyethane electrolyte solutions containing high concentrations of LiFSI at 1.6-2.3V vs. Li/Li^+ initiated by the FSI(–F) radical that is formed during reduction of LiFSI-based electrolyte solution at elevated temperatures. Based on QC calculations these authors proposed that the film formation occurs in the following process:

$(LiFSI)_2 + Li_2S_2 \rightarrow LiNS(O_2)S\text{-}SS(O_2)NLi + 2LiF$ (1)

The presence of the surface films was confirmed by SEM and XPS analysis. LiF and the decomposition products of LiFSI containing sulfonyl amide groups were detected on the surface of the electrodes.

In order to study the chemical composition of the surface films formed on the composite S-C electrodes in the IL electrolyte solution we performed XPS analysis. Fig.5 shows the high resolution F 1s, N 1s, C1s and S 2p spectra of a pristine electrode and a typical electrodes cycled at 30°C with two low cut off potentials: 1.7 and 1V and an electrode cycled at 60°C with a low cut off potential of 1V, in the IL electrolyte solution as indicated.

The F 1s spectrum of the pristine electrode shown in Fig. 5a contains a peak at 688.2 eV, which is associated with the PVdF binder [34]. In the C 1s spectrum of the pristine electrode peaks related to CF_2 (291.3 eV) and CH_2 (286.6 eV) carbon atoms were observed, as well as a signal of the carbon matrix and the carbon black at 284.8 eV. In the S 2p spectrum of the pristine electrode the doublet at 164.2 eV is related to the elemental sulfur [34].

The intensity of all of these peaks is considerably lower for the electrodes cycled down to 1.7 and 1V at 30°C suggesting the formation of surface films on the surface the electrodes, which mask the intrinsic signals of the electrodes. In parallel with the decrease of the signals corresponding to the components of the pristine electrodes, the growth of the total content of N, S and O was observed and the appearance of peaks related to components of the surface films was detected. The F 1s spectra of cycled electrodes contain signal of LiF at 685 eV [34]. The N1s spectra contain two peaks at 400.3 eV assigned to N^- atoms in FSI anions [35-38] and a peak at 398.9 eV, related to N^- atoms in an undefined (yet) product of FSI anions decomposition [33, 36, 37]. The S 2p spectrum of the electrode cycled at 30°C (green curve) shows peaks of two types of sulfur atoms in the surface films: a doublet at 168.2 eV and a non-resolved doublet at about 169.5eV. We suppose that the assignment of these signals may relate to the products of the polymerization reaction of LiFSI and Li_2S_2 (1) proposed by Kim et al. [33]. There are two types of sulfur atoms related to sulfonyl amide groups in the resulted products, namely, F-S*(O_2)-N- S(O_2)- with sulfur atoms connected to one F and one N atom, and F-S(O_2)-N-S*(O_2)- with sulfur atoms bounded to one S and one N atom. Possible assignment of the S atoms signals in light of the surface reaction proposed, is presented in Fig. 5d.

The composition of the surface species on electrodes cycled at 60°C is different. There is a strong indication that the surface films became thicker, since the signal of the carbon is substantially lower (Fig. 5c). The resulting surface films obviously contain less F-containing species (Fig. 5a). In the S2p spectra of the electrode cycled at the elevated temperature (Fig. 5d, black curve) one can observe the growth of the content of F-S*(O_2)-N- S(O_2)- (terminal) sulfur atoms in reference to F-S(O_2)-N-S*(O_2)- sulfur atoms. This observation relates to the average length of the polymeric chains in the surface film.

At the same time, the growth of C-N species (286.2 eV in C 1s spectrum) [34, 39] and N^+ species (the shoulder at about 402 eV in N 1s spectrum) [37] implies an increase of content of the decomposition products of MPP cations in the surface films at elevated temperature.

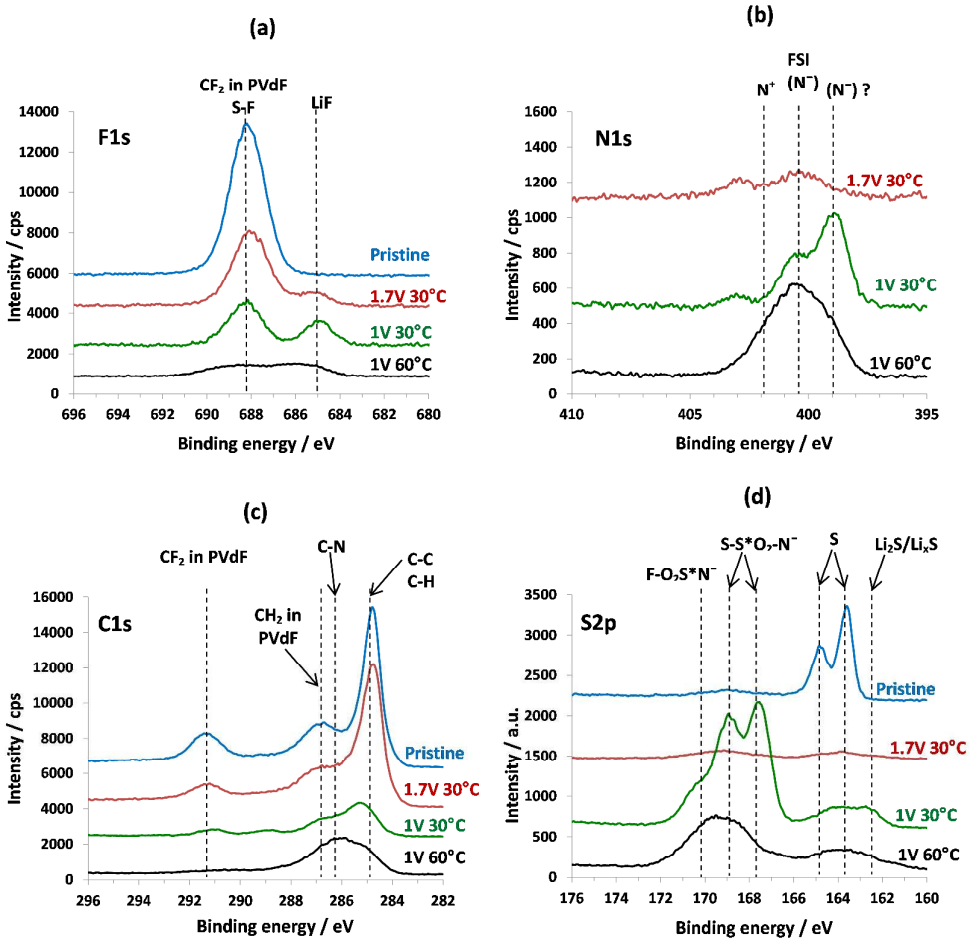

Fig. 5. F 1s (a), N 1s (b), C1s (c) and S 2p (d) XPS spectra of pristine composite S-C electrode (blue curves), S-C electrode cycled at 30°C with lower cut off potential value of 1.7V (red curves) and 1V (green curves) and the electrode cycled at 60°C with lower cut off potential value of 1V (black curves) in 0.5M Li FSI in MPP FSI electrolyte solution.

Thus, the results of the surface analysis suggest that during the cycling of S-C cathodes in the FSI-based IL electrolyte solution surface films (SEI) are formed. Obviously, the formation of SEI occurs during the initial discharge process when a high irreversible capacity is always observed. As we showed in [18], this pretreatment step at room temperature is a necessary condition for the following reversible cycling of S-C electrodes in this electrolyte solution. After the formation of the surface films in the initial cycles voltage differs of that commonly measured for Li-S systems and is characterized by single galvanostatic charge/discharge voltage plateau.

Analogous voltage profiles with potential hysteresis in the initial cycles and single voltage plateau in the subsequent cycling was reported for several types of carbon-sulfur composite electrodes and was observed generally for the organic carbonate-based electrolyte solutions. Wang et al. [7] explained this type of voltage response by the formation of special complexes of the sulfur embedded in the fine pores with carbon or surface-bonded oxygen. Therefore, the electrochemical reaction between sulfur and lithium during discharge will need an additional energy to break such complexes, leading to a high electrochemical polarization and a lower discharge voltage than pure sulfur. After lithium extraction, the complexes will reform but with a lower absorbing energy and the cell exhibits a higher discharge voltage after its first cycle. Zhang et al. [19] attributed similar voltage profiles to the unique micro-porous structure of carbon spheres as conductive matrix. They proposed that narrow micropores (≈ 0.7 nm) of carbon spheres can trap stably elemental sulfur, and subsequent lithium polysulfides during cycling due to a strong adsorption (complex formation). The strong adsorption interactions that may exist in that systems may avoid the detrimental shuttle mechanism, mass loss of the active materials and the formation of a thick insulating Li_2S layer on the composite cathode's surface. Thus, the electrochemical reaction is constrained only inside the narrow micropores. Xin et al. [20] also attributed a similar phenomenon to the microporous structure of the carbon matrix and suggested that metastable small sulfur molecules have been confined in the microporous carbon matrix with

pore size of ~0.5 nm. Indeed, cyclo-S_{5-8} with at least two dimensions large than 0.5 nm cannot exist inside, while small S_{2-4} molecules with at least one dimension less than 0.5 nm can be hosted therein. Wang et al. in [21, 22] suggested another possible mechanism for this phenomenon. Micropores below 1 nm force the desolvation of the electrolyte ions and thus prevent or slow down the dissolution of polysulfides as the solvent concentration is very low or close to zero in the micropores. Consequently the reduction of sulfur still produces polysulfides as intermediates, but the polysulfides remain in the pores instead of being dissolved. This suggests a quasi-solid-state reaction of the sulfur under solvent-deficient conditions. They stated that solvated ions tend to be desolvated in micropores with size close to the ion size. Thus, pore size is the key factor that facilitates the desolvation process.

Therefore, all the suggested models described above, explain the appearance of the anomalous behavior of S-C electrodes by the peculiarities of the porous structure of the carbon matrix.

The analysis of our results allows concluding that the model of the quasi-solid-state reaction in the pores of the activated carbon which occurs after Li ions desolvation [21, 22] suggested is very interesting. However, what was suggested so far ignored the importance of surface films formation and their involvement in the overall reactions.

In general, two types of behavior of S-C composite electrodes observed for different type of carbon-S composites and electrolyte solutions are schematically presented in Fig. 6. The first one (Fig. 6a) relates to the normal behavior of S-C electrodes with two discharge peaks observed in the standard voltammetric response of sulfur electrodes, and correspondingly, the two discharge plateaus observed in the galvanostatic voltage profiles. This type of behavior generally observed in all ethereal electrolyte solutions and is related to solid-liquid-solid reaction [22]. The second type of behavior called by Wang et al. “quasi-solid-state reaction” is presented in Fig. 6b. In our version based on the understanding achieved herein, this presentation is supplemented by emphasizing the critically important surface films which are formed in the initial discharge process and play a key role in the Li ions desolvation process. Therefore, for the realization of “quasi-solid-state reactions” of sulfur with Li ions in the pores of activated carbon matrices, the composition of the electrolyte solution and the protocol and procedure of the 1st discharge process in these systems are critically important. It is interesting that the formation of the surface films containing thiocarbonates on C/S composite cathodes was observed also in [24].

In support of this conclusion we can demonstrate that the same S-C composite electrodes exhibit different voltage profiles measured in two electrolyte solutions, namely, FSI-based IL and ethereal solution. We reported earlier on the cycling performance of S-AC1 composite cathodes with 50 wt. % S that was similar to what was described in the present work (Fig. 1, Fig.3, blue curves) in ethereal electrolyte solutions with LiTFSI salt [40-41]. Voltage profiles with two plateaus shown in

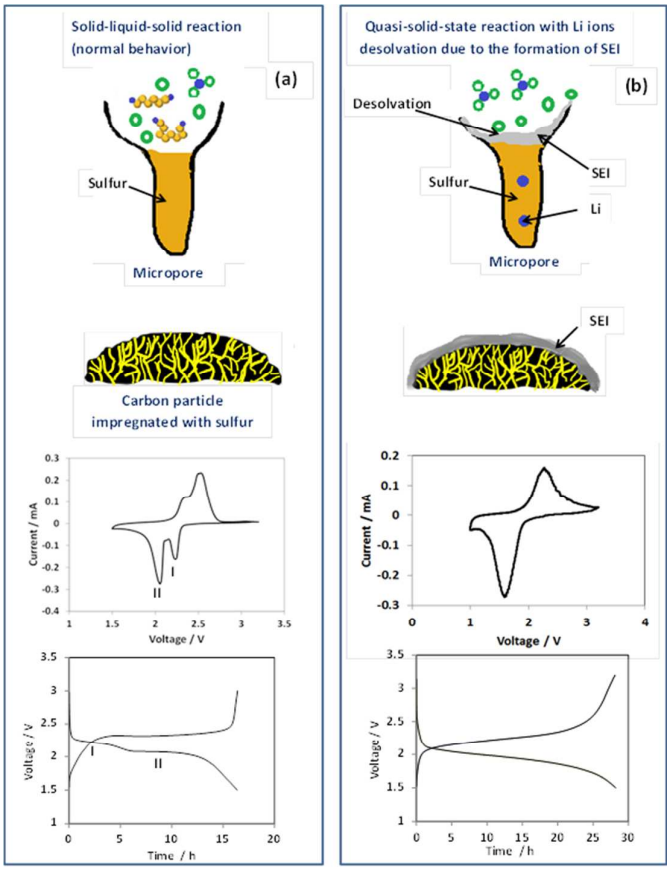

Fig. 6. Schematic presentation of the proposed mechanism, including quasi-solid-state reaction with Li ions desolvation due to the formation of SEI (b) in comparison to normally observed solid-liquid-solid reaction (a) and typical CV and galvanostatic response for both types of behavior of S-C electrodes.

these works relates to the first type of sulfur cathode behavior (normal behavior) presented in Fig. 6a. In the IL electrolyte solution used in the present work, the 2nd type of behavior, namely, voltage profiles with only one plateau, is observed due to the formation of SEI type surface films that fully separate between the sulfur confined in the carbon pores and the liquid electrolyte solution. Moreover, the electrodes after the pretreatment in which the SEI is formed, may be reversibly cycled in the electrolyte solutions in which they cannot work without the pretreatment. For example, in solutions based on propylene carbonate (PC) S-C electrodes fail due to the reactions of Li polysulfides with the carbonate molecules [42] (Fig.7a). However, after the pretreatment during several repeated cycles in the IL electrolyte solution (Fig. 7b) the electrodes transferred to the PC-based electrolyte solution demonstrated a stable cycling with voltage profiles showing only one plateau (Fig. 7c). Alternatively, normal voltage profiles with two plateaus observed the ethereal solutions (Fig. 7d) appeared when S-AC1 electrodes pretreated in the IL electrolyte solution (Fig. 7e) was transferred to this solution (Fig. 7f). It means that the SEI type surface films formed in the

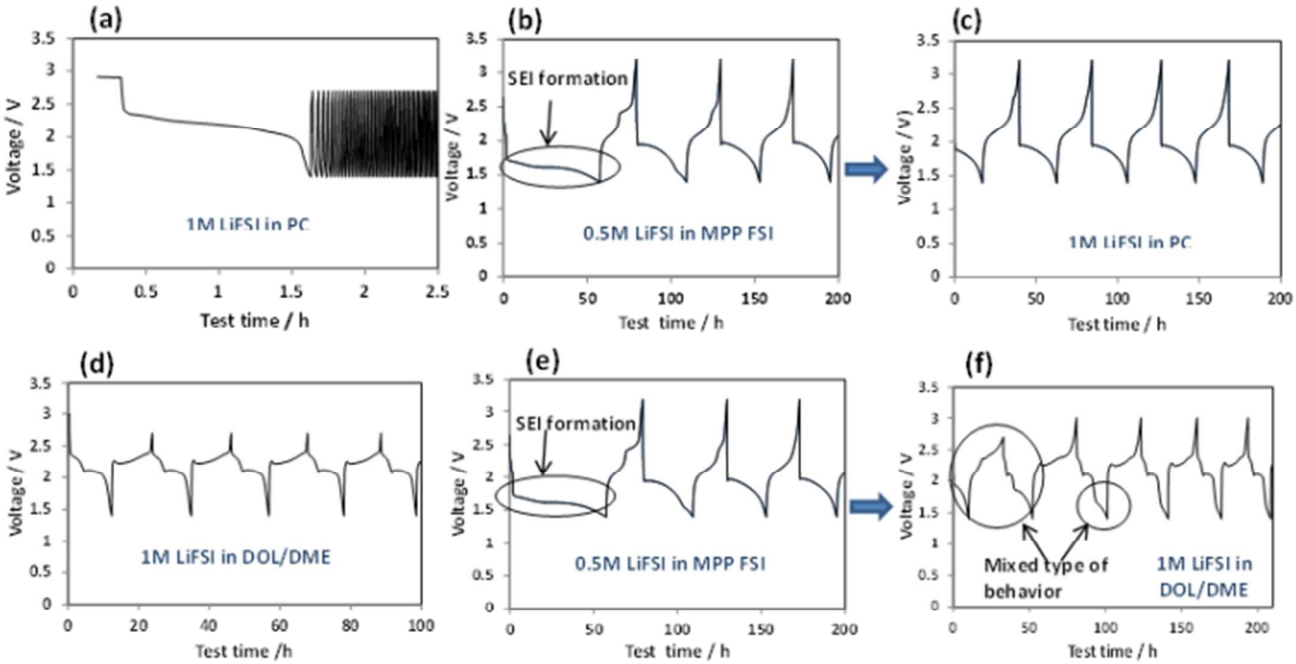

Fig. 7. Voltage profiles measured for composite S–C electrodes in PC-based and etheric electrolytes before and after the pretreatment step in IL electrolyte. (a) Fresh electrode cycled in 1M LiFSI in PC, (b) Fresh electrode cycled in 0.5M LiFSI in MPP FSI and (c) transferred after that to the new cell with fresh Li counter electrode and 1M Li FSI in PC electrolyte solution, (d) Fresh electrode cycled in 1M LiFSI in DOX/DME, (e) Fresh electrode cycled in 0.5M LiFSI in MPP FSI and (f) transferred after that to the new cell with fresh Li counter electrode and 1M LiFSI in DOX/DME electrolyte solution. Current density 50 mA g^{-1} sulfur, 30°C.

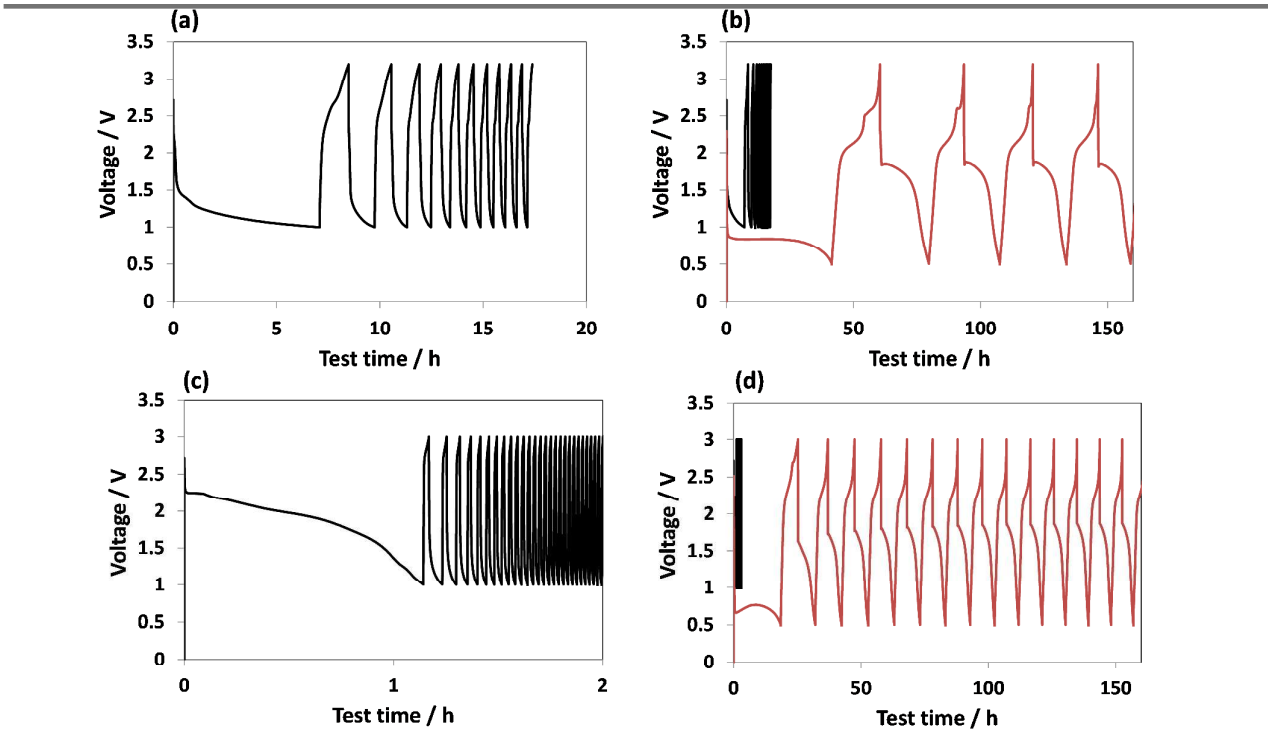

Fig. 8. Voltage profiles measured for composite S–C electrodes cycled with different discharge cut off voltage values in 0.5M LiTFSI in BMP TFSI (a, b) and 1M $LiPF_6$ in PC (c, d) electrolyte solutions. Current density 50 mA g^{-1} sulfur (a, b) and 100 mA g^{-1} sulfur (c, d), 30°C.

IL electrolyte solution (by the pretreatment) are not stable during cycling in 1M LiFSI/DOL/DME solutions, because the surface species dissolve in them. Finally, the effect of cycling conditions on the behavior of such electrodes may be demonstrated by the two following examples. As one can see, S-AC1 electrodes do not exhibit any activity in PC-based electrolyte solutions when cycled with a lower cut off voltage of 1.4V (Fig. 7a) and 1V (Fig. 8a and 8b, black curves). It is remarkable, that when the discharge of these electrodes was performed down to 0.5V, a reversible cycling with the 2nd type behavior (one plateau voltage profile) was observed (Fig. 8b). The same scenario was obtained for TFSI-based IL electrolyte solution (Fig. 8c, d).

These examples strongly support our conclusion that not a structure of the carbon matrix but rather the formation of protective surface films plays the key role in the operation of S-C electrodes via a quasi-solid-state mechanism.

Conclusions

We showed that the controlled formation of SEI type surface films on composite S-C electrodes affects their cycling performance and is responsible for the realization of quasi-solid-state mechanism of the electrochemical reaction of Li ions with sulfur encapsulated in microporous carbons. This type of behavior is characterized by voltage profiles which show only one plateau. The formation of SEI type surface films during the initial cycles is governed by the electrolyte solution composition and the discharge cut off voltage. Thus, the porous structure of the carbon host does not play a crucial role in the accomplishment of this type of reactions.

According to the proposed mechanism, cycling behavior of cells based on composite cathodes in which sulfur is encapsulated within activated carbon matrices, is highly dependent on the sulfur loading. Despite cracking of the particles observed due to a large volume expansion of sulfur during the lithiation, the best performance and initial Coulombic efficiency at room temperature in FSI-based IL electrolytes solutions was demonstrated by S-AC1 composite electrodes with sulfur loading of 60 wt. % . For this loading the micropores filled with sulfur are not accessible for N_2 molecules according to gas adsorption isotherm data. This sulfur loading prevents an access of electrolyte solution molecules to the micropores, and the quasi-solid-state reaction of Li ions with encapsulated sulfur occurs in solvent free environment.

SEI type surface films formed initially in the FSI-based IL electrolyte solutions remain stable in alkyl carbonate (PC) based solutions, but they are not stable (dissolve) in ethereal (DME/DOL) electrolyte solutions.

This insight into the mechanism of operating of S-C composite electrodes provides a new approach in the development of new electrolyte solutions and additives for Li-S cells. Besides, further optimization of C:S ratio and carbon host morphology in terms of porous structure and particle size is needed to achieve better cycling performance for these systems.

Notes and references

1 P. G. Bruce, B. Scrosati, J.-M. Tarascon, *Angew. Chem. Int. Ed*. 2008, **47**, 2930.
2 V. Etacheri, R. Marom, R. Elazari, G. Salitra, D. Aurbach, *Energy Environ. Sci.* 2011, **4**, 3243.
3 A. Manthiram, Y. Fu, S.-H. Chung, C. Zu, Y.-S. Su, *Chem. Rev.* 2014, **114**, 11751.
4 D.-W. Wang, Q. Zeng, G. Zhou, L. Yin, F. Li, H.-M. Cheng, I. R. Gentle, G. Q. M. Lu, *J. Mater. Chem. A* 2013, **1**, 9382.
5 A. Rosenman, E. Markevich, G. Salitra, D. Aurbach, A. Garsuch, F. F. Chesneau, *Adv. Energy Mater.* 2015, 1500212.
6 Y. V. Mikhaylik, J. R. Akridge, *J. Electrochem. Soc.* 2004, **151**, A1969.
7 J. L. Wang, J. Yang, J. Y. Xie, N. X. Xu, Y. Li, *Electrochem. commun.* 2002, **4**, 499.
8 X. Ji, K. T. Lee, L. F. Nazar, *Nat. Mater.* 2009, **8**, 500.
9 R. Elazari, G. Salitra, A. Garsuch, A. Panchenko, D. Aurbach, *Adv. Mater.* **2011**, *23*, 5641.
10 M.-S. Song, S.-C. Han, H.-S. Kim, J.-H. Kim; K.-T. Kim, Y.-M. Kang, H.-J. Ahn, S. X. Dou, J.-Y. Lee, *J. Electrochem. Soc*. 2004, **151**, A791.
11 Y. G. Zhang, Y. Zhao, A. Yermukhambetova, Z. Bakenov, P. J. Chen, *J. Mater. Chem. A* 2013, **1**, 295.
12 Y. J. Choi, B. S. Jung, D. J. Lee, K.W. Kim, H.J. Ahn, K.K. Cho, H.B. Gu, *Phys. Scr.* 2007, **T129**, 62.
13 S. Evers, T. Yim, L. F. Nazar, *J. Phys. Chem. C* 2012, **116**, 19653.
14 X. Ji, S. Evers, R. Black, L. F. Nazar, *Nat. Commun.* 2011, **2**, 325.
15 X. Liang, A. Garsuch, L. F. Nazar, *Angew. Chem. Int. Ed.* 2015, **54**, 3907.
16 J.-W. Park, K. Yamauchi, E. Takashima, N. Tachikawa, K. Ueno, K. Dokko, M. Watanabe, *J. Phys. Chem. C* 2013, **117**, 4431.
17 J.-W. Park, K. Ueno, N. Tachikawa, K. Dokko, M. Watanabe, *J. Phys. Chem. C* 2013, **117**, 20531.
18 G. Salitra, E. Markevich, A. Rosenman, Y. Talyosef, D. Aurbach, A. Garsuch, *ChemElectroChem* 2014, **1**, 1492.
19 B. Zhang, X. Qin, G. R. Li, X. P. Gao, *Energy Environ. Sci.* 2010, **3**, 1531.
20 S. Xin, L. Gu, N.-H. Zhao, Y.-X. Yin, L.-J. Zhou, Y.-G. Guo, L.-J. Wan, *J. Am. Chem. Soc.* 2012, **134**, 18510.
21 D.-W. Wang, G. Zhou, F. Li, K.-H. Wu, G. Q. M. (Max) Lu, H.-M. Cheng, I. R. Gentle, *Phys. Chem. Chem. Phys.* 2012, **14**, 8703.
22 D.-W. Wang, Q. Zeng, G. Zhou, L. Yin, F. Li, H.-M. Cheng, I. R. Gentle, G. Q. M. Lu, *J. Mater. Chem. A* 2013, **1**, 9382.
23 S. Zheng, P. Han, Z. Han, H. Zhang, Z. Tang, J. Yang, *Sci. Rep.* 2014, **4**, 4842.

24 Y. Xu, Y. Wen, Y. Zhu, K. Gaskell, K. A. Cychosz, B. Eichhorn, K. Xu, C. Wang, *Adv. Funct. Mater.* 2015, **25**, 4312.

25 W. Zhang, D. Qiao, J. Pan, Y. Cao, H. Yang, X. Ai, , *Electrochim. Acta* 2013, 87, 497.

26 Z. Li, L. Yuan, Z. Yi, Y. Sun, Y. Liu, Y. Jiang, Y. Shen, Y. Xin, Z. Zhang, Y. Huang, *Adv. Energy Mater.* 2014, **4**, 1301473.

27 Z. Peng, W. Fang, H. Zhao, J. Fang, H. Cheng, T. N. L. Doan, J. Xu, P. Chen, *Journal of Power Sources* 2015, **282**, 70.

28 S.S. Zhang, *Front. Energy Res.*, 2013, **1**, 10.

29 S.S. Zhang, *Energies* 2014, **7**, 4588.

30 Z. Lin, Z. Liu, N. J. Dudney, C. Liang, *ACS Nano* 2013, **7**, 2829.

31 Z. Lin, Z. Liu, W. Fu, N. J. Dudney, C. Liang, *Angew. Chem. Int. Ed. Engl.* 2013, **52**, 7460.

32 E. Markevich, M.D. Levi, D. Aurbach, *J. Electrochem. Soc.* 2005, **152**, A778.

33 H. Kim, F. Wu, J. T. Lee, N. Nitta, H.-T. Lin, M. Oschatz, W. I. Cho, S. Kaskel, O. Borodin, G. Yushin, *Adv. Energy Mater.* 2015, **5**, 1401792.

34 A. V. Naumkin, A. Kraut-Vass, S. W. Gaarenstroom, C. J. Powell, NIST X-ray Photoelectron Spectroscopy Database, NIST Standard Reference Database 20, Version 4.1. http://srdata.nist.gov/xps/(accessed June 1, 2015).

35 P. C. Howlett, N. Brack, A. F. Hollenkamp,c M. Forsyth, D. R. MacFarlane, *J. Electrochem. Soc.* 2006, **153**, A595.

36 B. Philippe, R. Dedryvere, M. Gorgoi, H. Rensmo, D. Gonbeau, K. Edström, *J. Am. Chem. Soc.* 2013, **135**, 9829.

37 A. Budi, A. Basile, G. Opletal, A. F. Hollenkamp, A. S. Best, R. J. Rees, A. I. Bhatt, A. P. O'Mullane, S. P. Russo, *J. Phys. Chem. C* 2012, **116**, 19789.

38 C. Liu, X. Ma, F. Xu, L. Zheng, H. Zhang, W. Feng, X. Huang, M. Armand, J. Nie, H. Chen, Z. Zhou, *Electrochim. Acta* 2014, **149**, 370.

39 N. K. Cuong, M. Tahara, N. Yamauchi, T. Sone, *Surf. Coat. Technol.* 2005, **193**, 283.

40 A. Rosenman, R. Elazari, G. Salitra, E. Markevich, D. Aurbach, A. Garsuch, *J. Electrochem. Soc.* 2015, **162**, A657.

41 A. Rosenman, R. Elazari, G. Salitra, D. Aurbach, A. Garsuch, *J. Electrochem. Soc.* 2014, **161**, A470.

42 J. Gao, M.A. Lowe, Y. Kiya, H.D. Abruna *J. Phys. Chem. C* 2011, **115**, 25132.

The formation of the surface films on sulfur-carbon cathodes is responsible for a quasi-solid-state mechanism of sulfur lithiation in the micropores.